Active-Site Mutations of the Diphtheria Toxin Catalytic Domain: Role of Histidine-21 in Nicotinamide Adenine Dinucleotide Binding and ADP-Ribosylation of Elongation Factor 2†

Steven R. Blanke,‡ Kathy Huang,‡ Brenda A. Wilson,‡,§ Emanuele Papini,‖ Antonello Covacci,⊥ and R. John Collier*,‡

Department of Microbiology and Molecular Genetics, Harvard Medical School, and The Shipley Institute of Medicine, Boston, Massachusetts 02115, CNR Biomembrane Center and General Pathology Institute, University of Padova, 35100 Padova, Italy, and Immunobiological Research Institute Siena, Via Fiorentina 1, 53100 Siena, Italy

Received December 22, 1993; Revised Manuscript Received February 23, 1994®

ABSTRACT: Diphtheria toxin (DT) has been studied as a model for understanding active-site structure and function in the ADP-ribosyltransferases. Earlier evidence suggested that histidine-21 of DT is important for the ADP-ribosylation of eukaryotic elongation factor 2 (EF-2). We have generated substitutions of this residue by cassette mutagenesis of a synthetic gene encoding the catalytic A fragment (DTA) of DT, and have characterized purified mutant forms of this domain. Changing histidine-21 to alanine, aspartic acid, leucine, glutamine, or arginine diminished ADP-ribosylation activity by 70-fold or greater. In contrast, asparagine proved to be a functionally conservative substitution, which reduced ADP-ribosylation activity by <3-fold. The asparagine mutant was approximately 50-fold-attenuated in NAD glycohydrolase activity, however. Dissociation constants (K_d) for NAD binding, determined by quenching of the intrinsic protein fluorescence, were 15 μM for wild-type DTA, 160 μM for the asparagine mutant, and greater than 500 μM NAD for the alanine, leucine, glutamine, and arginine mutants. These and previous results support a model of the ADP-ribosylation of EF-2 in which histidine-21 serves primarily a hydrogen-bonding function. We propose that the π-imidazole nitrogen of His-21 hydrogen-bonds to the nicotinamide carboxamide, orienting the N-glycosidic bond of NAD for attack by the incoming nucleophile in a direct displacement mechanism, and then stabilizing the transition-state intermediate of this reaction.

The expanding class of enzymes that catalyze mono-ADP-ribosylation reactions includes many bacterial toxins, as well as other enzymes of both prokaryotic and eukaryotic origin (Moss & Vaughan, 1990). Currently our understanding of catalytic mechanisms in these enzymes is limited, despite increasing evidence of their importance in various aspects of normal metabolism, as well as pathogenesis. Using diphtheria toxin (DT)[1] as a model for this class of biological catalysts, we have begun to define structural elements that dictate enzyme function.

DT is composed of three distinct structural domains, which function directly in the three steps of intoxication (Choe et al., 1992). After secretion from lysogenic strains of *Corynebacterium diphtheriae* carrying the phage-encoded *tox* gene, the toxin binds to the DT receptor and is internalized by the carboxyl-terminal domain (R domain) via receptor-mediated endocytosis (Naglich & Eidels, 1990; Naglich et al., 1992). The acidic environment of the endosome is believed to trigger a conformational change in the toxin, allowing the central domain (T domain) to insert into the endosomal membrane and the amino-terminal catalytic domain (C domain; equivalent to fragment A, or DTA) to be translocated across the membrane to the cytosol (Moskaug et al., 1991; Blewitt et al., 1985; Silverman et al., 1993). Two processing events, proteolytic cleavage at Arg-190, Arg-192, or Arg-193 and reduction of the disulfide linkage between cysteines-186 and -201, are required for release of DTA into the cytosol (Papini et al., 1993; Tsuneoka et al., 1993). As the final step in the intoxication pathway, DTA catalyzes the transfer of the ADP-ribose moiety of NAD to a posttranslationally modified histidine residue of elongation factor 2 (EF-2), called diphthamide (Van Ness et al., 1980). This covalent modification inactivates EF-2 and disrupts polypeptide chain elongation, resulting in cell death (Collier & Mekalanos, 1980; Collier, 1982; Collier & Traugh, 1969; Gill et al., 1969; Honjo et al., 1968).

Important structural details of the ADP-ribosylating toxins have begun to emerge recently, including the identities of important active-site residues. Glu-148 was identified as an active-site residue of DT by photoaffinity labeling experiments with NAD and subsequent site-directed mutagenesis studies (Carroll et al., 1980, 1985a; Carroll & Collier, 1984; Tweten et al., 1985; Wilson et al., 1990). Similar experiments with exotoxin A (ETA) from *Pseudomonas aeruginosa* revealed Glu-553 as an essential catalytic residue (Carroll & Collier, 1987; Douglas & Collier, 1990). These results implied that Glu-148 of DT and Glu-553 of ETA are functionally homologous residues, and provided an important reference

† This work was supported by NIH Grants AI-22021 and AI-22848 and by Postdoctoral Fellowship Awards NIH8469 (S.R.B.) and NIH8315 (B.A.W.).

* Author to whom correspondence should be addressed at the Department of Microbiology and Molecular Genetics, Harvard Medical School.

‡ Harvard Medical School and The Shipley Institute of Medicine.

§ Present address: Department of Biochemistry, Wright State University School of Medicine, Dayton, OH 45435.

‖ University of Padova.

⊥ Immunobiological Research Institute Siena.

® Abstract published in *Advance ACS Abstracts,* April 1, 1994.

[1] Abbreviations: ADP, adenosine 5′-diphosphate; BSA, bovine serum albumin; DEP, diethyl pyrocarbonate; DT, diphtheria toxin; EF-2, elongation factor 2; DTA, diphtheria toxin fragment A; DTT, dithiothreitol; EDTA, ethylenediaminetetraacetic acid; ETA, exotoxin A; NAD, nicotinamide adenine dinucleotide; TCA, trichloroacetic acid; Tris, tris(hydroxymethyl)aminomethane.

0006-2960/94/0433-5155$04.50/0

point for identification of sequence homology between the catalytic domains of these toxins (Carroll & Collier, 1988).

One of the interesting features that emerged from sequence comparisons of these two toxins was the conservation of His-21, the only histidine of DTA, as His-440 in ETA (Carroll & Collier, 1988). The crystal structures of these toxins now reveal that these residues are located in essentially identical positions within the active-site cleft of the catalytic domains (Choe et al., 1992; Allured et al., 1986). Other studies have suggested that NAD binds in close proximity to His-21 (Domenighini et al., 1991). Chemical modification of His-21 with diethyl pyrocarbonate (DEP) resulted in attenuation of DTA's ADP-ribosylating and NAD binding activities, suggesting an important role for this residue in catalysis (Papini et al., 1989, 1990).

Pursuant to a more detailed understanding of the role of His-21 in DTA function, this residue was changed by site-directed mutagenesis to alanine, aspartate, leucine, asparagine, glutamine, and arginine, using a recently completed synthetic gene encoding DTA (Blanke and Collier, unpublished data). Each of the mutants was overexpressed in *Escherichia coli*, purified to homogeneity, and analyzed for ADP-ribosylation activity, NAD glycohydrolase activity, and NAD binding. The results support the notion that His-21 forms part of the nicotinamide subsite of the NAD binding site and that it functions predominantly as a hydrogen bond donor, rather than a general base or nucleophile, in the ADP-ribosylation of EF-2.

EXPERIMENTAL PROCEDURES

Chemicals and Enzymes. All restriction endonucleases, deoxyribonucleotides, and T4 DNA ligase were purchased from New England Biolabs. Dideoxy sequencing kits were acquired from United States Biochemical. The nickel chelate chromatography resin and plasmid purification columns were obtained from Qiagen, Inc. Oligonucleotides encoding mutagenic codons at residue 21 were synthesized with an ABI Model 380A DNA synthesizer. [^{32}P]NAD (800 Ci/mmol) was purchased from Du Pont–New England Nuclear, and [4-^{3}H]NAD (2.7 Ci/mmol) was from Amersham.

Bacterial Strains and Plasmids. E. coli strain XL1-Blue was acquired from Stratagene, and BL21(DE3) was used for expression of proteins under transcriptional control of the T-7 promoter. The plasmids pUC19 and pET-15b were obtained from New England Biolabs and Novagen Inc., respectively.

Recombinant DNA Procedures. Standard protocols were utilized for isolation of plasmid DNA, restriction endonuclease digestions, subcloning, and transformation of *E. coli* (Ausubel et al., 1987).

Design and Construction of Mutant Cassettes. The strategy for generating the site-directed mutations at residue 21 is outlined in Figure 1. All of the genetic manipulations were performed in a synthetic gene encoding the structural gene for DTA, maintained in pUC19 (replacing the *Kas*I-*Hin*dIII fragment, New England Biolabs) (Blanke and Collier, unpublished data). The synthetic gene was designed by altering the codon usage of the corynephage β gene to reflect the bias exhibited by highly expressed proteins in *E. coli*. We divided the gene into smaller, evenly-spaced fragments by engineering unique restriction sites throughout the open reading frame. The His-21 mutations were encoded by synthetic cassettes, 85 base pairs in length, cloned into the *Pml*I–*Acc*I sites of the synthetic gene, comprising base number 50 to base number 134. Each synthetic cassette was constructed by annealing a pair of oligonucleotides with complementary sequences at the 3′ ends to form a short duplex element of 15 base pairs. The annealed oligos served as both primer and template for strand-extension with Sequenase, resulting in full-length double-stranded cassettes. The *Pml*I and *Acc*I restriction sites were 9 base pairs from the end of each cassette. The oligonucleotides were isolated with Oligonucleotide Purification Cartridges (Applied Biosystems), followed by further purification using denaturing polyacrylamide gel electrophoresis.

The synthetic cassettes were generated by annealing 25–100 pmol of each purified oligonucleotide. The oligonucleotides were incubated for 5 min at 80 °C, followed by 5 min at 40 °C (Figure 1). The annealed strands were extended in a 30-μL reaction mixture of 5 mM dithiothreitol (DTT), 250 μM deoxynucleotides, and 50 μg/mL bovine serum albumin (BSA). The extension reactions were initiated by the addition of 13 units of Sequenase; reaction mixtures were incubated at 37 °C for 30 min, followed by incubation at 70 °C for 20 min. The mixture was diluted to 200 μL using water and restriction digestion buffer (New England Biolabs), and the appropriate restriction sites were generated by a *Pml*I–*Acc*I double digestion for 4–8 h. The DNA was ethanol-precipitated and resolved using 10% nondenaturing polyacrylamide gel electrophoresis. The appropriate sized synthetic cassettes were excised from the gel, and the DNA was eluted overnight by two serial elutions in 2.5 M sodium acetate at 37 °C and concentrated by ethanol precipitation. The two precipitates were resuspended in water and combined. Half of this mixture was cloned directly into the Pm*l*I and *Acc*I sites of the synthetic gene. The ligation reactions were transformed into *E. coli* XL1-Blue. Plasmid DNA from transformed colonies was screened using Sequenase version 2.0, and those genes possessing the appropriate mutant codon 21 were further subcloned into the expression vector pET-15b (replacing the *Nco*I–*Bam*HI fragment, Novagen) and transformed into the expression strain BL21(DE3).

Fermentation and Harvest of E. coli. A single 50-mL culture of L-broth (100 mg/mL ampicillin) was inoculated with a single colony from an LB-amp plate freshly streaked with BL21(DE3) transformed with pET-15b-DTA. This inoculum was grown to an OD = 0.5 (600 nm) and then placed at 4 °C overnight. On the second day, 2-L baffled flasks, each containing 500 mL of L-broth (100 mg/mL ampicillin) prewarmed to 37 °C, were inoculated with 5 mL of the 50-mL overnight culture. The flasks were aerated on a rotary shaker at 37 °C. The cultures were induced at an OD_{600} = 1.0 with 1–2 mM isopropyl β-D-thiogalactopyranoside (IPTG). The cells were harvested after 1–2 h, immediately chilled to 4 °C, and centrifuged at 3000*g* for 10 min at 4 °C. The pellets were resuspended in 5 mL of ice-cold sonication buffer, composed of 50 mM Na_2HPO_4, pH 8.0, 100 mM KCl, 0.1% Tween-20, 1.0 mM phenylmethanesulfonyl fluoride, and 20 mM β-mercaptoethanol. The resuspended pellets were either frozen at −70 °C or sonicated immediately.

Purification of Mutant Toxins. The combined pellets were sonicated 3 times for 30–45 s, using a Sonifier Cell Disruptor 350 (Branson Sonic Power Co.), with the power control at 5 and the duty cycle at 50%. The extracts were chilled on ice for at least 1 min between each sonication cycle. Cellular debris was pelleted by centrifuging at 3500*g* for 20 min at 4 °C. The supernatants were collected and chilled, while the pellets were resuspended in 5–10 mL of sonication buffer and sonicated again as described above.

The synthetic gene encoding DTA was designed with an N-terminal fusion peptide of six histidines, used for nickel

chelate affinity chromatography. The crude extracts were clarified immediately before chromatography by centrifuging at 20000*g* for 15 min. The extracts were adjusted to 12 mM imidazole, and then loaded directly onto a 3–5-mL nickel chelate affinity column (Qiagen), preequilibrated with 5 bed volumes of sonication buffer. The column was washed with 3 bed volumes of sonication buffer plus 12 mM imidazole, followed by 3–5 bed volumes of sonication buffer plus 20 mM imidazole. The purified proteins were eluted with 5 bed volumes of sonication buffer plus 50 mM imidazole. The column fractions were analyzed by sodium dodecyl sulfate (SDS)–polyacrylamide gel electrophoresis, and the purified protein was pooled.

Proteolytic Removal of the Polyhistidine Fusion Peptide. Typically, 1 mg of toxin was incubated with 2–5 units of human thrombin (Novagen) for 1–5 days at 20 °C in 20 mM Tris-HCl, pH 8.4, 150 mM NaCl, and 2.5 mM $CaCl_2$. The intact DTA was purified using a single anion-exchange FPLC chromatography fractionation step (Mono Q from Pharmacia).

Protease Digestions. Relative stabilities of the mutant proteins to that of wild-type toxin were assessed by analysis of the protein's stability to limited proteolytic digestion with trypsin and chymotrypsin. In parallel reactions, each protein (5–10 μg) was incubated with 5–100 ng of trypsin or chymotrypsin in a total volume of 30 μL of 10 mM Tris-HCl, pH 7.5, containing 20 mM DTT, for 1–2 h at 25 °C. The reactions were stopped by the addition of 20 μL of SDS–polyacrylamide sample buffer containing BME and heating at 90 °C for 2 min, followed by analysis on a 15% denaturing SDS–polyacrylamide gel.

NAD–EF-2 ADP-Ribosyltransferase Assay. The NAD–EF-2 ADP-ribosyltransferase assay measures the initial rates of incorporation of the [^{32}P]NAD ADP-ribose moiety of NAD into the trichloroacetic acid (TCA)-precipitable EF-2 fraction of the reaction mixture. The assay was modified so that initial rates were determined by the collection of 3–4 linear time points in duplicate rather than the collection of a single time point in duplicate (Wilson et al., 1990). Reactions in a final volume of 50 μL of 50 mM Tris-HCl, pH 8.0, 1 mM EDTA, 10 mM DTT, and 50 μg of BSA/mL, and the specified concentrations of NAD and EF-2 for each experiment, were incubated with DTA at 25 °C. Assays were also performed in 50 mM MES–KOH, pH 6.0, and 50 mM HEPES–KOH, pH 7.0. Generally, aliquots were removed from duplicate samples at 2, 3, 4, and 5 min and pipetted directly onto TCA-saturated 3MM filter paper (Whatman). The filter pads were placed immediately into ice-cold 5% TCA and washed 3–5 times for 15 min by gently agitating on a platform rocker until no counts could be detected in the discarded wash solutions. The filter pads were then washed twice for 5 min in ice-cold methanol, dried, and counted with 3 mL of Beckman Ready Safe Liquid Scintillation Cocktail in a 1209 Rackbeta scintillation counter (LKB). Initial rates were calculated on the basis of the increase in counts (minus background) over 5 min with less than 10% of the reactants having been utilized.

NAD Glycohydrolase Assay. The initial rates of NAD glycohydrolysis by DTA were determined by the hydrolysis of [*nicotinamide*-4-^{3}H]NAD. The assay was typically conducted over 4 h at 25 °C in a final volume of 200 μL of 50 mM Tris-HCl, pH 8.2, 1 mM EDTA, 5 mM DTT, and 50 μg/mL BSA. Aliquots were collected at 1, 2, 3, and 4 h by transferring 45 μL into 30 μL of 0.5 M sodium borate buffer, pH 8.0, which was subsequently extracted with 200 μL of water-saturated ethyl acetate. A 150-μL sample of the organic phase was removed and counted in 3 mL of Beckman Ready Safe Liquid Scintillation Cocktail. All data were adjusted for the nonenzymatic hydrolysis of NAD.

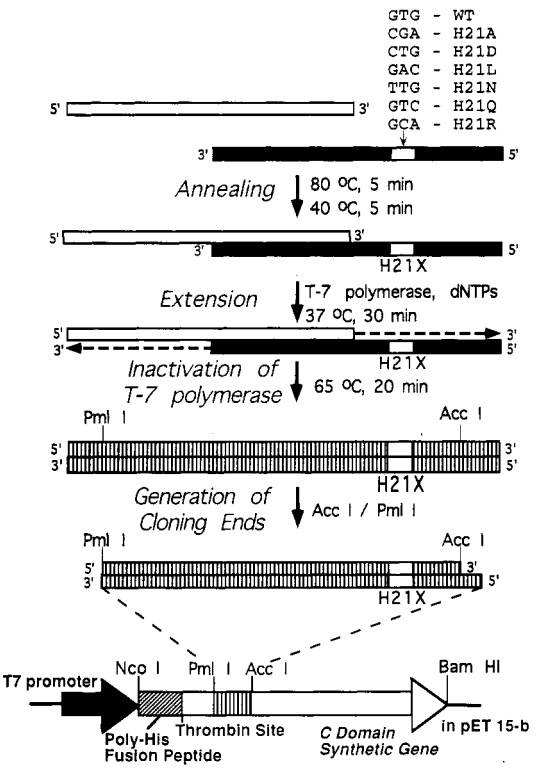

FIGURE 1: Protocol for construction of mutations at residue 21. Synthetic cassettes were generated by annealing two self-priming oligonucleotides, extension of the strands with Sequenase version 2.0, and generation of the appropriate restriction sites by *PmlI–AccI* double digestions. The DNA was ethanol-precipitated and resolved using 10% nondenaturing polyacrylamide gel electrophoresis. The appropriate sized synthetic cassettes were excised from the gel, and the DNA was eluted overnight by two serial elutions in 2.5 M sodium acetate at 37 °C, and concentrated by ethanol precipitation. The two precipitates were resuspended in water and combined, and a portion of this mixture was cloned directly into the *PmlI* and *AccI* sites of the synthetic gene.

Fluorescence Quenching. The determination of NAD binding by the quenching of intrinsic toxin fluorescence at pH 8.0 and 25 °C was performed as previously described (Wilson et al., 1990).

RESULTS

Production of Wild-Type and Mutant Proteins. Substitutions for His-21 were generated by cloning synthetic mutant cassettes between the *PmlI* and *AccI* sites of an entirely synthetic gene encoding DTA plus a 17-residue amino-terminal hexahistidine fusion peptide (Figure 1) (Blanke and Collier, unpublished results). Each mutant protein, cloned into *NcoI–BamHI* sites of the expression vector pET-15b, was completely sequenced. The proteins were expressed in the *E. coli* strain BL21(DE3) by activation of the T7 RNA polymerase with IPTG and were initially purified by nickel chelate chromatography. The amino-terminal hexahistidine fusion peptides were removed enzymatically with thrombin, and the authentic proteins were then further purified by anion-exchange chromatography FPLC. Protein purity was greater than 95%, as estimated by SDS–PAGE. Relative protein stabilities were determined by incubation with trypsin and chymotrypsin, followed by analysis of the products by SDS–PAGE. H21D was the only mutation that markedly enhanced sensitivity to these proteases.

ADP-Ribosylation Activity of Mutant Proteins. The ADP-ribosylation activity was estimated for each mutant protein

Table 1: Comparison of Specific Activities for ADP-Ribosylation by Wild-Type and Mutant DTA Enzymes[a]

toxin	specific activity[b]	relative specific activity
wild type	1200 ± 70	1.0 (1/1)
H21N	470 ± 60	0.39 (1/2.6)
H21R	18 ± 1	0.015 (1/67)
H21Q	11 ± 1	0.0092 (1/110)
H21A	10 ± 1	0.0083 (1/120)
H21L	5.6 ± 0.6	0.0047 (1/210)
toxin	**pH[c]**	**relative specific activity**
wild type	6.0, 7.0	1.0 (1/1)
H21N	7.0	0.64 (1/1.8)
H21N	6.0	1.2 (1/0.83)

[a] All assays were performed under the following conditions: 50 mM Tris-HCl, pH 8.0, 1 mM EDTA, 10 mM DTT, 50 μM NAD, and 2.5 μM EF-2, at 25 °C. The values were generated from at least three assays performed in duplicate. [b] Defined as the number of moles of EF-2 ADP-ribosylated per minute per mole of enzyme. [c] Assays were performed under the following conditions: 50 mM MES–KOH, pH 6.0, or 50 mM HEPES–KOH, pH 7.0, with 1 mM EDTA, 10 mM DTT, 50 μM NAD, and 2.0 μM EF-2, at 25 °C.

Table 2: Comparison of Specific Activities for NAD Glycohydrolase by Wild-Type and Mutant DTA Enzymes[a]

toxin	specific activity[b]	relative specific activity
wild type	$(6.9 \pm 0.4) \times 10^{-3}$	1.0 (1/1)
H21N	$(1.5 \pm 0.4) \times 10^{-4}$	0.022 (1/46)
H21R	$(1.3 \pm 0.5) \times 10^{-4}$	0.019 (1/53)
H21A	$<6.9 \times 10^{-5}$	<0.010 (<1/100)
H21L	$<6.9 \times 10^{-5}$	<0.010 (<1/100)
H21Q	$<6.9 \times 10^{-5}$	<0.010 (<1/100)

[a] Assays are run at 25 °C. Reaction mixtures contain 50 μM NAD, 50 mM Tris-HCl, pH 8.2, 1 mM EDTA, 5 mM DTT, and 50 μg/mL BSA. Initial velocities were obtained from at least three separate experiments, each performed in duplicate. [b] Defined as the number of moles of NAD hydrolyzed per minute per mole of enzyme.

by measuring initial rates at 50 μM NAD, 2.5 μM EF-2, pH 8.0, and 25 °C (Table 1). In contrast to the H21A, H21L, H21Q, and H21R mutants, all of which showed reductions of 70-fold or greater, H21N retained a relatively high percentage of wild-type activity—ca. 40%. As H21D caused instability, initial rates could not be measured accurately for this mutant; however, in repeated measurements, the activity of the mutant was never greater than 1% of the wild-type control.

The ADP-ribosylation activities of wild-type DTA and H21N were also measured at pH values lower than 8.0 (Table 1). At pH 7.0, H21N exhibited 64% of wild-type activity, while at pH 6.0, H21N exhibited slightly higher activity (120%) than wild-type DTA.

NAD Glycohydrolase Activity of Mutant Proteins. In the absence of EF-2, DTA hydrolyzes NAD to nicotinamide and ADP-ribose at a slow but measurable rate, a reaction with no known physiological significance. Relative specific activities in the NAD glycohydrolase reaction were determined from initial rates of [^{3}H]nicotinamide release, at 50 μM NAD, pH 8.0, and 25 °C. All of the mutant proteins exhibited profoundly lowered activity (Table 2). H21N and H21R both retained approximately 2% of wild-type activity, whereas H21A, H21L, and H21Q demonstrated less than 1% of wild-type activity.

Effects of Mutations on NAD Binding. The diminished ADP-ribosylation and NAD glycohydrolase activities of the His-21 DTA mutants suggested that NAD binding may be altered. The dissociation constants (K_d) of NAD binding were measured by quenching of the intrinsic protein fluorescence at pH 8.0 and 25 °C (Wilson et al., 1990). Substituting

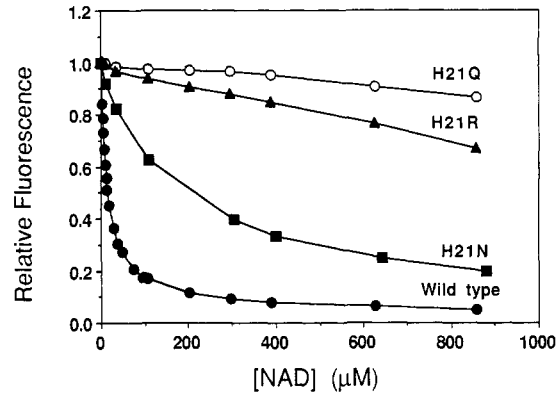

FIGURE 2: Quenching of intrinsic protein fluorescence for DTA-WT, DTA-H21N, DTA-H21Q, and DTA-H21R by NAD. The assays were performed as previously described (Wilson et al., 1990), by titrating with NAD at 25 °C. The plots are from single fluorescence quenching experiments, which were repeated at least 4 times for DTA-WT and DTA-H21N, and at least 2 times for DTA-H21Q and DTA-H21R. The percent quenching at each NAD concentration was calculated from the data and analyzed by Hanes plots to determine the dissociation constants for the wild-type and mutant proteins. The K_d values are summarized in Table 3.

Table 3: Comparison of Dissociation Constants and Binding Energies for NAD Binding to Wild-Type and Mutant DTA Enzymes[a]

toxin	K_d (μM)[b]	difference in binding energies ($\Delta\Delta G_S$, kcal/mol)[c]
wild type	15.1 ± 1.4	
H21N	163 ± 14	1.4
H21A	*d*	>3
H21L	*d*	>3
H21Q	*d*	>3
H21R	*d*	>3

[a] Experiments were performed as previously described in Wilson *et al.* (1990). [b] Determined from Hanes plot analysis of the percent fluorescence quenching as a function of NAD concentration. The values were generated from the average of at least four assays. [c] Determined from the difference in the Gibb's free energy, $\Delta G_S = RT \ln K_d$, obtained for NAD binding to the mutant and wild-type enzymes. [d] Could not be determined since <30% of the protein's fluorescence was quenched at concentrations of NAD up to 860 μM.

arginine or glutamine for His-21 greatly reduced the ability of DTA to bind NAD, while the asparagine mutation caused less drastic alterations (Figure 2). The K_d for NAD binding to H21N was 160 μM, compared to 15 μM for wild-type DTA (Table 3). K_d values for H21A, H21L, H21R, and H21Q could not be accurately measured, as there was minimal quenching of intrinsic DTA fluorescence, even at 900 μM NAD, indicating that the substrate bound poorly to these mutant proteins. The differences in binding energies for NAD binding in the ground-state binary complex were determined from the dissociation constants, according to the equation

$$\Delta G_S = RT \ln K_d$$

The ground-state binding energy was 1.4 kcal/mol higher for the H21N mutant (–5.2 kcal/mol) compared to that of wild-type DTA (–6.6 kcal/mol), while the difference in binding energy of the other mutants was estimated to be much greater than 3 kcal/mol (Table 3).

Kinetic Studies. Following initial measurements of ADP-ribosylation activity, which showed that the H21N mutation allowed retention of substantial levels of activity, while other mutations caused major losses, we selected H21N and H21Q for more extensive kinetic studies. NAD concentrations were

Table 4: Kinetics of ADP-Ribosyltransferase Activity[a]

toxin	k_{cat} (min^{-1})	K_m(NAD) (μM)	k_{cat}/K_m (min^{-1} M^{-1})	$\Delta G_{apparent}$ (kcal/mol)
wild type	3800	52	7.4×10^7	
H21N	1200	79	1.5×10^7	+0.95
H21Q	100	480	2.1×10^5	+3.46

[a] All assays are the average of at least two assays performed in duplicate. Assay conditions were 3–250 μM NAD, 2.5 μM EF-2, 50 mM Tris-HCl, pH 8.0, 1 mM EDTA, 10 mM DTT, and 50 μg/mL BSA. Reactions were run at 25 °C.

varied from 2 to 450 μM, and kinetic parameters were determined from either Lineweaver–Burk or Hanes–Woolf plots (Table 4). The Michaelis constant (K_m) for H21N was determined to be 79 μM NAD, compared to 52 μM for wild-type DTA. H21N exhibited only a 3–4-fold decrease in the turnover number, k_{cat}. However, the K_m for H21Q was 480 μM, while the k_{cat} was also reduced substantially, from 3900 to 100 min^{-1}. The catalytic efficiency (k_{cat}/K_m) for H21N was approximately one-fifth that for the wild-type enzyme, but was reduced by a factor of approximately 350 for H21Q.

The change in apparent binding energy (ΔG) from mutating residues that interact with the transition-state intermediate of the ADP-ribosylation reaction can be determined from the ratio of k_{cat}/K_m (Wilkinson et al., 1983; Carter et al., 1984; Fersht, 1987a), with

$$\Delta G = -RT \ln[(k_{cat}/K_m)_{mutant}/(k_{cat}/K_m)_{wild\ type}]$$

The apparent free energy change from substituting glutamine for histidine was +3.5 kcal/mol, while the apparent change from substituting asparagine for histidine was only +0.95 kcal/mol (Table 4).

DISCUSSION

In recent years, the active site of DT has been studied as a useful model for understanding structure–function relationships in ADP-ribosyltransferases. The most extensively studied residue in this site is Glu-148, which was originally identified by photoaffinity labeling with NAD. This residue appears to be broadly conserved in the ADP-ribosyltransferases, and directed mutagenesis studies have shown Glu-148 and its homologs in other toxins to be essential for the ADP-ribosylation reaction. Glu-148 in DTA has been proposed to activate diphthamide to serve as the incoming nucleophile in a direct displacement reaction (Oppenheimer & Bodley, 1981; Chung & Collier, 1977; Wilson et al., 1990); Wilson & Collier, 1992; Tweten et al., 1985). Besides Glu-148, Tyr-65 and His-21 of DTA have received the most attention in regard to the catalytic function. These three residues are all close to each other within the active-site cleft. Photolabeling studies with 8-azidoadenine and 8-azidoadenosine by Papini et al. (1991), combined with other results, led the authors to propose that Tyr-65 interacts with the nicotinamide ring of NAD (Domenighini et al., 1991). Papini et al. (1989, 1990) also demonstrated that modification of His-21 with diethyl pyrocarbonate diminished both ADP-ribosylation and NAD binding activities, suggesting an important role of this residue in catalysis.

To probe the role of His-21 in substrate binding and catalysis, we originally constructed a number of point mutations in the DTA gene cloned from corynebacteriophage β and expressed them in *E. coli*. Preliminary characterization of the mutant proteins in crude extracts suggested that all the substitutions, with the exception of asparagine, caused major reductions in ADP-ribosyltransferase activity (Blanke et al., 1992). However, further characterization of the precise role of His-21 in catalysis was hampered by our inability to obtain sufficient amounts of pure protein from the corynephage gene in *E. coli*, due to its low level of expression in this system. Consequently, we were led to construct an entirely synthetic gene for DTA, more amenable to our goal (Blanke et al., unpublished data). As a result, we were able to perform a more detailed analysis of the function of His-21, using mutant and wild-type DTA proteins produced from this gene. The data presented here confirm and refine our earlier observations, and, additionally, define the effects of the His-21 mutations on NAD binding and NAD glycohydrolysis.

The first step in the ADP-ribosylation and NAD hydrolysis reactions is the binding of NAD to form the binary, ground-state complex (Kandel et al., 1974; Collier et al., 1974; Chung & Collier, 1977; Collier, 1982). Substitution of His-21 with arginine (H21R), leucine (H21L), alanine (H21A), or glutamine (H21E) drastically diminished both ADP-ribosyltransferase and NAD glycohydrolase activities. The asparagine mutation (H21N), on the other hand, showed little effect on ADP-ribosylation activity (<3-fold), while causing a 50-fold decrease in NAD glycohydrolysis. Fluorescence quenching experiments indicated that the attenuated enzymatic activities of all the mutants, except H21N, are primarily due to the toxin's decreased ability to recognize and bind NAD. The K_d values were all significantly greater than 500 μM, compared to 15 μM for wild-type protein. In contrast, replacement with asparagine (H21N) yielded a K_d value of 160 μM, only 10-fold higher than that of wild-type DTA. The ground-state binding energy, estimated from the observed K_d values, was 1.4 kcal/mol higher for the H21N mutant (–5.2 kcal/mol) compared to that of wild-type DTA (–6.6 kcal/mol), and the difference in binding energy of the other mutants was estimated to be much greater than 3 kcal/mol since very little NAD binding was detectable by fluorescence quenching. These results support the notion that His-21 plays an important role in NAD binding and that histidine and asparagine interact with NAD in a similar manner in the initial toxin–NAD complex.

The fact that asparagine can effectively substitute for His-21 in the ADP-ribosylation of EF-2 further suggests that it is not the acid–base properties of histidine but rather its hydrogen-bond-forming ability that is important for catalysis. Lowe et al. (1985) have compared the imidazole nitrogens of histidine to the side-chain carboxamide nitrogens of asparagine and glutamine, observing that the amide δ-nitrogen of asparagine is approximately isosteric to the π-nitrogen of the imidazole ring of histidine, while the amide ϵ-nitrogen of glutamine is approximately isosteric to the τ-nitrogen (Figure 3). Since asparagine was found to serve as a much better substitute than glutamine, we propose that it is the π-nitrogen of His-21, and not the τ-nitrogen, that is involved in hydrogen-bonding with NAD.

While crystallographic studies of NAD binding have not yet yielded a model of this dinucleotide in the active-site cleft of DT (or of any other ADP-ribosyltransferase), various data suggest that His-21 forms part of the nicotinamide subsite. In an early model of NAD binding to the active-site cleft of ETA, proposed by Brandhuber et al. (1988), the nicotinamide ring was hypothesized to stack on the side chain of Trp-466 (corresponding to Trp-50 in DT), while the adenine ring interacted with the phenolic ring of Tyr-481 (corresponding to Tyr-65 of DT). This arrangement was inconsistent with the results of experiments by Carroll and co-workers (Carroll

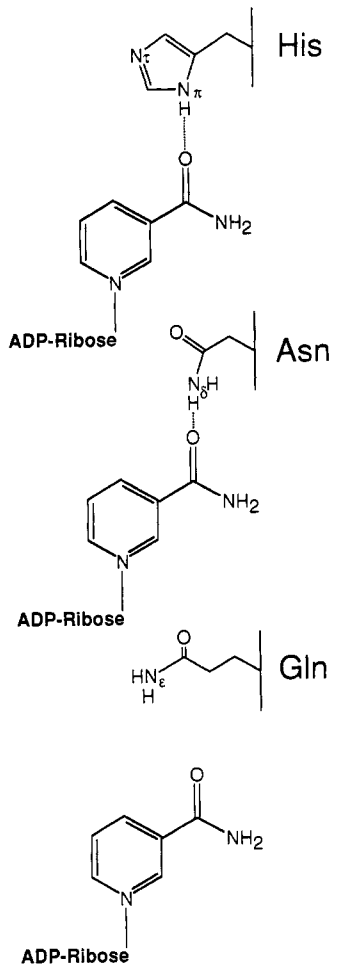

FIGURE 3: Model of how the approximate equivalence between the π-nitrogen of His-21 and the δ-amide group of Asn-21 allows both residues to hydrogen-bond with the nicotinamide carboxyamide moiety of NAD. The substitution of glutamine for His-21 introduces a long side chain that disrupts hydrogen-bonding interactions, and causes further perturbations in the NAD binding site.

& Collier, 1984; Carroll et al., 1985a,b), however, in which NAD was used as a photoaffinity label with DT or ETA. The structure of the photoproduct formed, which contains the entire nicotinamide moiety of NAD covalently linked through C-6 to the decarboxylated γ-methylene carbon of Glu-148 in DT, suggested that the side chain of this moiety must be in close proximity to the N-glycosidic bond that is cleaved during the ADP-ribosylation and NAD glycohydrolase reactions. Subsequently, the photolabeling studies by Papini et al. (1991) with 8-azidoadenine and 8-azidoadenosine led the authors to suggest a model in which NAD assumed effectively the opposite orientation—namely, with the nicotinamide ring stacked onto the phenolic ring of Tyr-65 and the adenine ring on Trp-50. Besides being more consistent with the photo-induced linking of nicotinamide to Glu-148, this model is supported by the crystallographic structure of the endogenous dinucleotide adenylyl-3′,5′-uridine monophosphate, which binds tightly (and competitively with NAD) to the active site of DTA (Choe et al., 1992). The uridine ring of adenylyl-3′,5′-uridine monophosphate, which may be considered to be an analog of the nicotinamide ring of NAD, is positioned in a pocket formed between the imidazole ring of His-21 and the phenolic ring of Tyr-65, which are coplanar and approximately 7 Å apart. It is thus a reasonable assumption that the nicotinamide ring of NAD binds in approximately the same location, and therefore in close proximity to the imidazole ring of His-21.

If this model is correct, His-21 may function primarily by hydrogen-bonding to the carboxamide group of the nicotinamide moiety of NAD, thereby serving to orient the nicotinamide ring and the nicotinamide–ribose linkage. The ADP-ribose reaction has been proposed to proceed by a direct displacement reaction, with the π-imidazole nitrogen of diphthamide being activated by Glu-148 for nucleophilic attack on the N-glycosidic bond of NAD (Wilson et al., 1990; Wilson & Collier, 1992). Although the latter bond is highly activated for hydrolysis (ΔG = 8.2 kcal/mol) (Zatman et al., 1953), there is considerable rotational freedom of the nicotinamide ring around the N-glycosidic bond relative to the adjacent ribose ring. Aromatic interaction of the nicotinamide ring with the phenolic side chain of Tyr-65, coupled with hydrogen-bonding of the amide group to the imidazole of His-21, could limit both rotational and translational freedom, and provide for a more favorable orientation of the N-glycosidic bond for nucleophilic attack. Precise orientation is likely to be crucial, since local substrate conformational effects can have profound effects on the electronic nature of the transition state (Horenstein & Schramm, 1993; Fersht, 1987b), and conformational effects imposed by enzymic groups can influence the developing charge distribution for stabilization of the transition state (Horenstein & Schramm, 1993; Fersht, 1987b; Venanzi et al., 1992; Sjoberg & Politzer, 1990; Lamotte-Brasseur et al., 1990). It is not clear whether the positive charge on the imidazole ring of His-21 makes any contribution toward substrate binding in the transition state, but previous results indicated that there was an acidic, active-site group, presumably His-21, with a pK_a of about 6.3, whose titration was influenced by the presence or absence of Glu-148 (Wilson et al., 1990). We have additionally observed that the 2.5-fold reduced ADP-ribosyltransferase activity for the H21N mutant could be brought up to wild-type levels by reducing the pH of the reaction from 7.5–8.0 to less than 7.0 (Table 1).

Since His-21 is required for both binding and catalysis, as determined from our kinetic measurements, this residue must be important for interacting with substrate both in the initial ground-state complex and in the transition-state complex. As stated earlier, we propose that this interaction primarily involves hydrogen bond formation with the amide group of nicotinamide, although there may be a small electronic contribution as well. The binding energy contribution of a single hydrogen bond by an uncharged histidine residue has been estimated to stabilize the transition state of an enzyme-catalyzed reaction by 0.5–1.8 kcal/mol (Fersht et al., 1985; Fersht, 1987b). Kinetic analysis revealed that the glutamine substitution (H21Q) destabilized the transition state by 3.5 kcal/mol, suggesting that this mutation not only disrupts hydrogen-bonding contacts with the nicotinamide carboxamide but also produces additional perturbations in the active site. By comparison, mutating His-21 to asparagine (H21N) destabilized the transition state by only 0.95 kcal/mol. Richardson and Richardson (1989) have observed that both of the imidazole nitrogens of histidine residues tend to be involved in hydrogen bonding within the interior of a protein. The slight destabilization of the asparagine substitution may reflect the loss of a hydrogen bond between the τ-nitrogen of the imidazole ring of histidine and the transition-state intermediate.

Despite its ability to substitute effectively in the ADP-ribosylation of EF-2, asparagine proved not to be a conservative substitution for His-21 in the single-substrate NAD glycohydrolase reaction. A detailed kinetic analysis of the NAD glycohydrolase reaction was not performed for our mutants,

but the substantial reduction in NAD recognition and binding shown by fluorescence quenching data must be at least partly responsible for this reduction in activity. The absence of a similar large effect of the H21N mutation on the ADP-ribosylation of EF-2 suggests that the presence of EF-2 must stabilize the ternary complex and sterically prevent dissociation of NAD.

ADDED IN PROOF

Another group has independently found that DTA-H21N retained a significant level of ADP-ribosylation activity, whereas mutating His-21 to any other residue virtually abolished activity (Johnson & Nicholls, 1994).

ACKNOWLEDGMENT

We acknowledge Angela Vilche for excellent technical assistance, and Susan Martinis, Jill Milne, Philip Hanna, Cesare Montecucco, and Rino Rappuoli for useful discussions and critical reading of the manuscript.

REFERENCES

Allured, V. S., Collier, R. J., Carroll, S. F., & McKay, D. B. (1986) *Proc. Natl. Acad. Sci. U.S.A. 83*, 1320.

Ausubel, F., Brent, R., Kingston, R. E., Moore, D. D., Seidman, J. G., Smith, J. A., & Struhl, K. (1987) in *Current protocols in molecular biology*, John Wiley and Sons, New York.

Blanke, S. R., Collier, R. J., Covacci, A., Fu, H., Killeen, K., Montecucco, C., Papini, E., Rappuoli, R., & Wilson, B. A. (1992) in *Bacterial Protein Toxins, Fifth European Workshop* (Witholt, B., Alouf, J. E., Boulnois, G. J., Cossart, P., Dijkstra, B. W., Falmagne, P., Fehrenbach, F. J., Freer, J., Niemann, H., Rappuoli, R., & Wadstrom, T., Eds) pp 349–354, Gustav Fischer Verlag, New York.

Blewitt, M. G., Chung, L. A., & London, E. (1985) *Biochemistry 24*, 5458.

Brandhuber, B. J., Allured, V. S., Falbel, T. G., & McKay, D. B. (1988) *Proteins: Struct., Funct., Genet. 3*, 146.

Carroll, S. F., & Collier, R. J. (1984) *Proc. Natl. Acad. Sci. U.S.A. 81*, 3307.

Carroll, S. F., & Collier, R. J. (1987) *J. Biol. Chem. 262*, 8707.

Carroll, S. F., & Collier, R. J. (1988) *Mol. Microbiol. 2*, 293.

Carroll, S. F., Lory, S., & Collier, R. J. (1980) *J. Biol. Chem. 255*, 12020.

Carroll, S. F., McCloskey, J. A., Crain, P. F., Oppenheimer, N. J., Marschner, T. M., & Collier, R. J. (1985a) *Proc. Natl. Acad. Sci. U.S.A. 82*, 7237.

Carroll, S. F., Oppenheimer, N. J., Marschner, T. M., McCloskey, J. A., Crain, P. F., & Collier, R. J. (1985b) in *ADP-Ribosylation of Proteins* (Althaus, F. R., Hilz, H., & Shall, S., Eds.) pp 544–550, Springer-Verlag, New York.

Carter, P. J., Winter, G., Wilkinson, A. J., & Fersht, A. R. (1984) *Cell 38*, 835.

Choe, S., Bennett, M., Fujii, G., Curmi, P. M. G., Kantardjieff, K. A., Collier, R. J., & Eisenberg, D. (1992) *Nature 357*, 216.

Chung, D. W., & Collier, R. J. (1977) *Biochim. Biophys. Acta 483*, 248.

Collier, R. J. (1982) in *ADP-Ribosylation Reactions* (Hayaishi, O., & Ueda, K., Eds.) pp 575–592, Academic Press, New York.

Collier, R. J., & Traugh, J. A. (1969) *Cold Spring Harbor Symp. Quant. Biol. 34*, 589.

Collier, R. J., & Mekalanos, J. J. (1980) in *Multifunctional Proteins* (Bisswanger, H., & Schmincke-Ott, E., Eds.) pp 261–291, John Wiley & Sons, New York.

Collier, R. J., DeLange, R. J., Drazin, R., Kandel, J., & Chung, D. W. (1974) in *Poly(ADP-Ribose), An International Symposium* (Harris, M., Ed.) pp 287–304, DHEW Publication No. (NIH) 74–477, U.S. Government Printing Office, Washington, D.C.

Domenighini, M., Montecucco, C., Ripka, W. C., & Rappuoli, R. (1991) *Mol. Microbiol. 5*, 23.

Douglas, C. M., & Collier, R. J. (1990) *Biochemistry 29*, 5043.

Fersht, A. R. (1987a) *Biochemistry 26*, 1577.

Fersht, A. R. (1987b) *Trends Biochem. Sci. 12*, 301.

Fersht, A. R., Shi, J. P., Knill-Jones, J., Lowe, D. M., Wilkinson, A. J., Blow, D. M., Brick, P., Carter, P., Waye, M. M., & Winter, G. (1985) *Nature 314*, 235.

Gill, D. M., Pappenheimer, A. M., & Baseman, J. B. (1969) *Cold Spring Harbor Symp. Quant. Biol. 34*, 595.

Honjo, T., Nishizuka, Y., & Hayaishi, O. (1968) *J. Biol. Chem. 243*, 3553.

Horenstein, B. A., & Schramm, V. L. (1993) *Biochemistry 32*, 7089.

Johnson, V. G., & Nicholls, P. (1994) *J. Biol. Chem. 269*, 4349.

Kandel, J., Collier, R. J., & Chung, D. W. (1974) *J. Biol. Chem. 249*, 2088.

Lamotte-Brasseur, J., Dive, G., Dehareng, D., & Ghuysen, J. M. (1990) *J. Theor. Biol. 145*, 183.

Lowe, D. M., Fersht, A. R., Wilkinson, A. J., Carter, P., & Winter, G. (1985) *Biochemistry 24*, 5106.

Moskaug, J. O., Stenmark, H., & Olsnes, S. (1991) *J. Biol. Chem. 266*, 2652.

Moss, J., & Vaughn, M. (1990) in *ADP-Ribosylating Toxins and G Proteins: Insights into Signal Transduction*, Library of Congress, Washington, D.C.

Naglich, J. G., & Eidels, L. (1990) *Proc. Natl. Acad. Sci. U.S.A. 87*, 7250.

Naglich, J. G., Metherall, J. E., Russell, D. W., & Eidels, L. (1992) *Cell 69*, 1051.

Oppenheimer, N. J., & Bodley, J. W. (1981) *J. Biol. Chem. 256*, 8579.

Papini, E., Schiavo, G., Sandona, D., Rappuoli, R., & Montecucco, C. (1989) *J. Biol. Chem. 264*, 12385.

Papini, E., Schiavo, G., Rappuoli, R., & Montecucco, C. (1990) *Toxicon 28*, 631.

Papini, E., Santucci, A., Schiavo, G., Domenighini, M., Neri, P., Rappuoli, R., & Montecucco, C. (1991) *J. Biol. Chem. 266*, 2494.

Papini, E., Rappuoli, R., Murgia, M., & Montecucco, C. (1993) *J. Biol. Chem. 268*, 1567.

Richardson, J. S., & Richardson, D. C. (1989) in *Prediction of Protein Structure and the Principles of Protein Conformation* (Fasman, G. D., Ed.) pp 1–98, Plenum Press, New York.

Silverman, J. A., Mindell, J. A., Finkelstein, A., & Collier, R. J. (1993) *J. Membr. Biol.* (in press).

Sjoberg, P., & Politzer, P. (1990) *J. Phys. Chem. 94*, 3959.

Tsuneoka, M., Nakayama, K., Hatsuzawa, K., Komada, M., Kitamura, N., & Mekada, E. (1993) *J. Biol. Chem. 268*, 26461.

Tweten, R. K., Barbieri, J. T., & Collier, R. J. (1985) *J. Biol. Chem. 260*, 10392.

Van Ness, B. G., Howard, J. B., & Bodley, J. W. (1980) *J. Biol. Chem. 255*, 10710.

Venanzi, C. A., Plant, C., & Venanzi, T. J. (1992) *J. Med. Chem. 35*, 1643.

Wilkinson, A. J., Fersht, A. R., Blow, D. M., & Winter, G. (1983) *Biochemistry 22*, 3581.

Wilson, B. A., & Collier, R. J. (1992) *Curr. Top. Microbiol. Immunol. 175*, 27–41.

Wilson, B. A., Reich, K. A., Weinstein, B. R., & Collier, R. J. (1990) *Biochemistry 29*, 8643.

Zatman, L., Kaplan, N., & Colowick, S. (1953) *J. Biol. Chem. 200*, 1974.